296 Novel Design of a 4 DOF Parallel Robot

V. SANGVERAPHUNSIRI[1)], N. TANTAWIROON[2)]

This work illustrates the novel design of a unique 4 degree-of –freedom parallel robot with 3 DOF in translation and one DOF in rotation. The forward and inverse kinematics will be detailed including the analysis of the singularities of the mechanism. The extensive simulation of the system is proposed. The design methodology shows the advantage over the other conventional method in less complexity of the direct kinematics solutions which can be extended to 5 or 6 DOF parallel robot. The purpose configuration can be applied to the rapid prototype application and also the 5-axis milling machine for advance manufacturing application.

Keywords: Parallel Configuration Robot, Singularity, Forward Kinematics, Inverse Kinematics, Automation, Safety.

1. INTRODUCTION

Parallel robots have been the topics of research for many years since Gough and Stewart, due to the advantages over serial robot such as more load capacity, stiffness and precision, speed and acceleration. Some of these robots are HexaM, and Toyoda. The potential application of Parallel mechanisms manipulator ranging from high-speed machining applications in machine tool industries such machines are Fanuc, Giddings & Lewis to the very complicated simulator using in the space applications. The aforementioned parallel robots have many configurations based on 3 to 6 degrees of freedom, such as the 3 degrees of freedom translation robot and a 6 degrees of freedom fully parallel robot which has 3 degrees of freedom for translation and another 3 degrees of freedom for rotation. These 6-dof robots normally consist of two platforms moving in relative, one is fixed called the base and the other is moving. Two platforms are connected to each other by chains of mechanism called leg or limb. These chains may have one degree of freedom with universal or spherical passive joints, or a chain of 2 degrees of freedom such as in purposed in ref [1]. One should consult ref [2] for better understanding about allowable actuated and passive joints to form a fully parallel robot of desired degree of freedom. Most of the current development works in parallel robot are concerning the design and development of new "family" of parallel mechanism, such as famous Delta robot [3], H-4 robot [4]. The analytical solutions and computation results for forward kinematics or singularity analysis of both robots are explain in [5], [6], and [7]. Undeniably, most research effort have been put into 6-degree of freedom parallel robot because of complex characteristics. Many researchers ([3], [4], [8]) aim for machine that has less than 6-dof which, in fact, capable for most industrial applications such as complicated machining required 5-axis and pick-and-place applications required at least 4-dof (3 in translation and one in rotation).The hexapod suffer complex kinematics when using its 6-dof in machining applications which require 5-axis and because of the limited workspace and tilting angle, its large structures cannot be avoided. The purpose of this research is to design and analyze parallel structure that has less complexity and has good performance in applications such as machining and reverse engineering (use of high resolution camera to scan 3-D surface) and force control manipulator arm.

2. DESIGN CONSIDERATIONS

The desired parallel robot must have at least 4-dof with 3 in translation and 1 in rotation. The robot should have large rotation angle. The design consists of two mechanical chains connect to the moving platform. The chains are independent at both sides of the machine along the x-axis. The workspace is depends on 4 parameters as the length of limb, R, the size of platform, c, the difference between machine frame and platform, (b – a). From this configuration, the constant-rotation workspace is up to the allowable distance in linear motion of the x-axis, the mobility of platform is uniformly distributes through out the working volume. Fig. 2 shows cross-section (y-z plane) of the working volume for some specified tilting angle. This illustrates one the good characteristic of this configuration that the tilting angle has very small effect to the change of working volume. This is not the case in typical Stewart platforms.

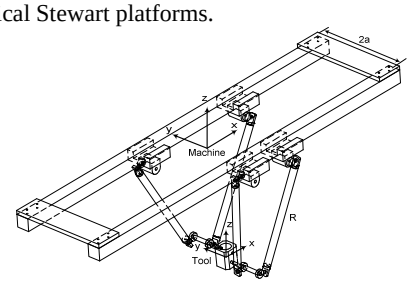

Figure (1) Proposed design

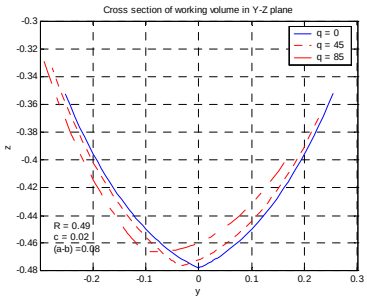

Figure (2) workspace at constant tilting angle at 0^{o}, 45^{o}, and 85^{o}

3. KINEMATICS MODELING

In this section, we derive the relationships between actuator's and moving platform's positions represented by $\mathbf{q} = [l_1 \quad l_2 \quad l_3 \quad l_4]$ and $\mathbf{x} = [x \quad y \quad z \quad \theta]^T$ respectively.

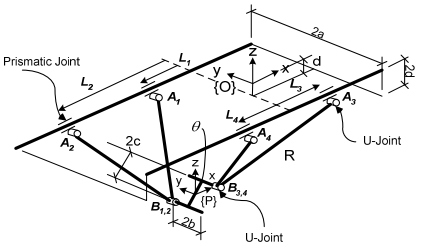

Figure (3) The proposed Configuration

From figure (3), inverse position relationships can easily be obtained as follow,

---

* Presentation at 2003 JSAE Annual Congress

1), 2) Faculty of Engineering, Chulalongkorn University, Bangkok, Thailand, 10330

For joint $i = 1,2$

$$\mathbf{A_iB_i} = \mathbf{p_1} - \mathbf{l_1}$$

or

$$\left\|\mathbf{A_iB_i}\right\|^2 = \left\|\mathbf{p_1} - \mathbf{l_1}\right\|^2$$

Where

$$\mathbf{x} = \begin{bmatrix} \mathbf{p} & \boldsymbol{\theta} \end{bmatrix}^T$$

$$\mathbf{p_1} = \mathbf{p} + \begin{bmatrix} -c\cdot\sin\boldsymbol{\theta} & b-a & d-c\cdot\cos\boldsymbol{\theta} \end{bmatrix}^T$$

The above equations will lead to,

$$l_1 = x_1 \pm \sqrt{R^2 - {y_1}^2 - {z_1}^2}$$

But from geometrical restrictions, we can conclude that

$$l_1 = x_1 + \sqrt{R^2 - {y_1}^2 - {z_1}^2} \qquad (1)$$

$$l_2 = x_1 - \sqrt{R^2 - {y_1}^2 - {z_1}^2} \qquad (2)$$

Similarly, the others actuator-end effecter position relationship become,

$$l_3 = x_2 + \sqrt{R^2 - {y_2}^2 - {z_2}^2} \qquad (3)$$

$$l_4 = x_2 - \sqrt{R^2 - {y_2}^2 - {z_2}^2} \qquad (4)$$

Where

$$\mathbf{p_2} = \mathbf{p} + \begin{bmatrix} c\cdot\sin\boldsymbol{\theta} & a-b & -d+c\cdot\cos\boldsymbol{\theta} \end{bmatrix}^T$$

In case of forward, position relationship can be obtained by manipulating expression 1, 2, 3 and 4 which lead to,

$$(l_1 - x_1)^2 + (l_3 - x_2)^2 = 2R^2 - 2y^2 - 2(b-a)^2 - 2z^2 - 2(d - c\cdot\cos\boldsymbol{\theta})^2 \qquad (a)$$

$$(l_2 - x_1)^2 - (l_4 - x_2)^2 = -4y(b-a) - 4z(d - c\cdot\cos\boldsymbol{\theta}) \qquad (b)$$

Which finally, we will obtain

$$y = \frac{(l_2 - x_1)^2 - (l_4 - x_2)^2 + 4z(d - c\cdot\cos\boldsymbol{\theta})}{4(a-b)}$$

For simpler expression, we defined new variables as shown in figure (4),

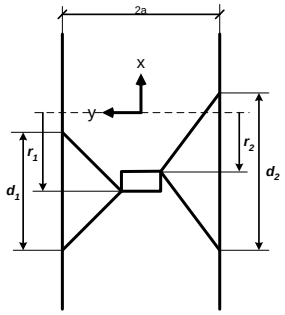

Figure (4) new variables defined

$$(l_2 - x_1)^2 = (l_1 - x_1)^2 = \frac{d_1^2}{4}$$

$$(l_4 - x_2)^2 = (l_3 - x_2)^2 = \frac{d_2^2}{4}$$

So,

$$x = \frac{r_1 + r_2}{2} \qquad (5)$$

$$y = \frac{d_1^2 - d_2^2 + 16z(d - c\cdot\cos\boldsymbol{\theta})}{16(a-b)}$$

And

$$\cos\boldsymbol{\theta} = \frac{\sqrt{4c^2 - (r_2 - r_1)^2}}{2c} \qquad (6)$$

Solution for y becomes,

$$y = \frac{d_1^2 - d_2^2 + 8z\left(2d - \sqrt{4c^2 - (r_2 - r_1)^2}\right)}{16(a-b)} \text{ --- (7)}$$

We can obtain z by substitutes the above expression in (b), which leading to 2nd degree polynomial equation as:

$$\frac{(d_1^2 + d_2^2)}{4} - 2R^2 + 2(b-a)^2 + 2\left(d - \frac{\sqrt{4c^2 - (r_2 - r_1)^2}}{2}\right)^2 + \frac{(d_1^2 - d_2^2)^2}{128(a-b)^2} +$$

$$z\frac{(d_1^2 - d_2^2)\left(2d - \sqrt{4c^2 - (r_2 - r_1)^2}\right)}{8(a-b)^2} + \qquad (8)$$

$$z^2\left(\frac{4\left(d^2 + c^2\right) - (r_2 - r_1)^2 - 4d\sqrt{4c^2 - (r_2 - r_1)^2}}{2(a-b)^2} + 2\right) = 0$$

In case of velocity relationship, by obtaining the relationship of the velocity of the moving platform and the actuator input as following:

Moving platform velocity,

$$\mathbf{V_{Bi}} = \mathbf{V_P} + \boldsymbol{\omega} \times \mathbf{PB_i}$$

Then, the velocity at point B related to that of point A,

$$\mathbf{A_iB_i} \bullet \mathbf{V_{Ai}} = \mathbf{A_iB_i} \bullet \mathbf{V_{Bi}}$$

According to [5], the Jacobian matrix of the parallel manipulator can be written in the form as

$$\mathbf{A}\dot{\mathbf{q}} = \mathbf{B}\dot{\mathbf{x}}$$

So,

$$\mathbf{A_iB_i} \bullet \mathbf{V_{Ai}} = \mathbf{A_iB_i} \bullet \mathbf{V_P} + \left(\mathbf{A_iB_i} \times \mathbf{PB_i}\right) \bullet \dot{\boldsymbol{\theta}}\mathbf{j}$$

$$\mathbf{A} = \begin{bmatrix} \mathbf{A_1B_1} \bullet \mathbf{i} & 0 & 0 & 0 \\ 0 & \mathbf{A_2B_2} \bullet \mathbf{i} & 0 & 0 \\ 0 & 0 & \mathbf{A_3B_3} \bullet \mathbf{i} & 0 \\ 0 & 0 & 0 & \mathbf{A_4B_4} \bullet \mathbf{i} \end{bmatrix}$$

$$\dot{\mathbf{q}} = \begin{bmatrix} \dot{l}_1 & \dot{l}_2 & \dot{l}_3 & \dot{l}_4 \end{bmatrix}^T$$

$$\mathbf{B} = \begin{bmatrix} \mathbf{A_1B_1} & \left(\mathbf{A_1B_1} \times \mathbf{PB_1}\right) \bullet \mathbf{j} \\ \mathbf{A_2B_2} & \left(\mathbf{A_2B_2} \times \mathbf{PB_2}\right) \bullet \mathbf{j} \\ \mathbf{A_3B_3} & \left(\mathbf{A_3B_3} \times \mathbf{PB_3}\right) \bullet \mathbf{j} \\ \mathbf{A_4B_4} & \left(\mathbf{A_4B_4} \times \mathbf{PB_4}\right) \bullet \mathbf{j} \end{bmatrix}$$

$$\dot{\mathbf{x}} = \begin{bmatrix} x & y & z & \boldsymbol{\theta} \end{bmatrix}^T \qquad (9)$$

At this point one can analyze the singularity configuration of the manipulator by, according to [5], [1] finding the determinant of matrix **A** and **B**. In this case we interests in singularity of type 2 [5] which occurs within workspace. From the set of equations (9) substitute all parameters into the matrix yield,

$$\mathbf{B} = \begin{bmatrix} x_1 - l_1 & y_1 & z_1 & \begin{bmatrix} x_1 - l_1 & z_1 \end{bmatrix}\mathbf{u_1} \\ x_1 - l_2 & y_1 & z_1 & \begin{bmatrix} x_1 - l_2 & z_1 \end{bmatrix}\mathbf{u_1} \\ x_2 - l_3 & y_2 & z_2 & \begin{bmatrix} x_2 - l_3 & z_2 \end{bmatrix}\mathbf{u_2} \\ x_2 - l_4 & y_2 & z_2 & \begin{bmatrix} x_2 - l_4 & z_2 \end{bmatrix}\mathbf{u_2} \end{bmatrix} \qquad (10)$$

Where,

$$\mathbf{u_1} = \begin{bmatrix} -c\cdot\cos\boldsymbol{\theta} & c\cdot\sin\boldsymbol{\theta} \end{bmatrix}^T$$

$$\mathbf{u_2} = \begin{bmatrix} c\cdot\cos\boldsymbol{\theta} & -c\cdot\sin\boldsymbol{\theta} \end{bmatrix}^T$$

The analytical form of the determinant of matrix **B** is found to be,

$$\det(\mathbf{B}) = 2\cdot c\cdot(l_1 - l_2)\cdot(l_3 - l_4)\cdot\cos\boldsymbol{\theta}\cdot\left[2y(d - \cos\boldsymbol{\theta}) - 2z(b-a)\right] \qquad (11)$$

From observation of (11), singularity occurs at following cases,

1) $l_1 - l_2$ or $l_3 - l_4$ is zero. This indicate that lines $\mathbf{A_1B_1}$ and $\mathbf{A_2B_2}$ or $\mathbf{A_3B_3}$ and $\mathbf{A_4B_4}$ are coincide.

2) $\cos\theta = 0$ or $\theta = \pm 90^\circ$. This means that the moving platform is parallel to x-axis.

3) $y(d - \cos\theta) - z(b - a) = 0 \Rightarrow z = \frac{y(d - \cos\theta)}{(b - a)}$, which shows that the planes formed by lines $\mathbf{A_1B_1}$ and $\mathbf{A_2B_2}$ and by $\mathbf{A_3B_3}$ and $\mathbf{A_4B_4}$ are in parallel.

(1), (2)

(3)

Figure (5) Singularity Configurations

4. SIMULATION RESULTS

This section we will show the simulation results of the feedback control by using the derived kinematics equations. The control scheme implemented in the simulations is based on joint space and Cartesian space. The Matlab/Simulink® will be used for the control law implementation and the MSC.VisualNastran® will be used for representing virtual plant behavior. Noting that with joint space control scheme, one should be careful with actual platform path which may cross into the singular region results in the undesired behavior.

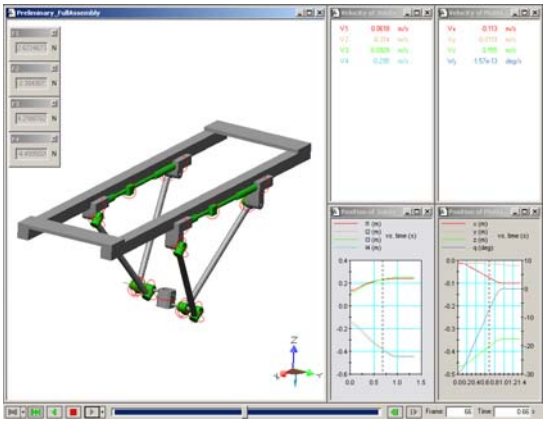

Figure (6) MSC.visualNastran workspace

As for joint space control, as shown in the fig. (7), we assign PID control with position feedback for individual joint. In case of Cartesian space, as shown in the fig. (8), we generate path for the platform motion using linear and parabolic blending in addition of control signal consist of position, velocity feedback and integral term from which, for ideal case, the actual moving platform trajectory should exactly match the desired trajectory with no error, given the control law,

$$F = \mathbf{M(x,l)} \cdot \ddot{l} + \mathbf{K_D}\left(\dot{l} - \dot{l}_d\right) + \mathbf{K_P}\left(l - l_d\right) + \mathbf{K_I}\int\left(l - l_d\right)dt$$

$$F = \mathbf{M(x,l)} \cdot \ddot{l} + \mathbf{K_D}\dot{e} + \mathbf{K_P}e + \mathbf{K_I}\int e dt$$

Where $\mathbf{l_d}$ is the desired joint positions.
Let testing by assign the conditions as
Start point: $x = -0.01\ y = -0.016\ z = -0.467\ \theta = 29^\circ$
End point: $x = -0.1\ y = -0.05\ z = -0.38\ \theta = 0^\circ$

Fig. 9 and fig 10 show the simulation results of the positions and velocities of the moving platform, fig. 9, and of the actuated joints, fig. 10, using the joint space control scheme, fig. 7. The simulation result illustrates very promising control scheme.

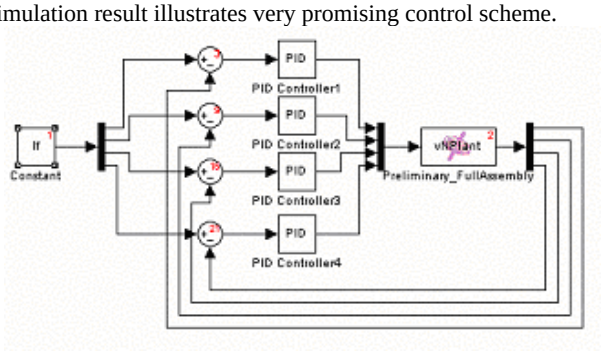

Figure (7) Joint space control scheme

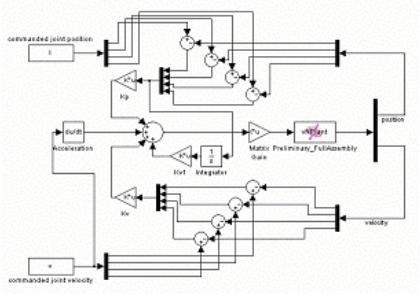

Figure (8) Cartesian space control scheme

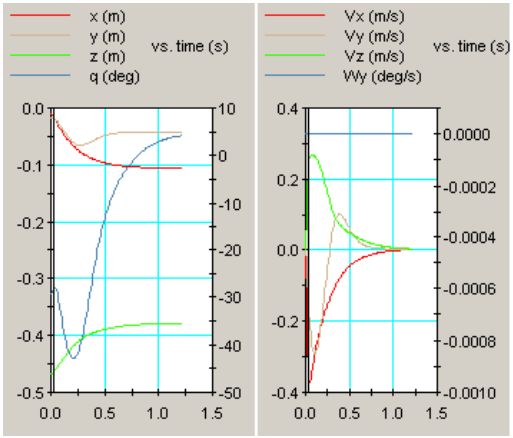

Figure (9) Positions and velocities of the moving platform using joint space control scheme

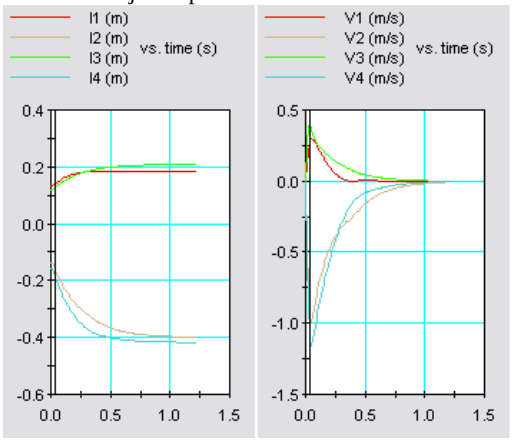

Figure (10) Positions and velocities of the actuated joints using joint space control scheme

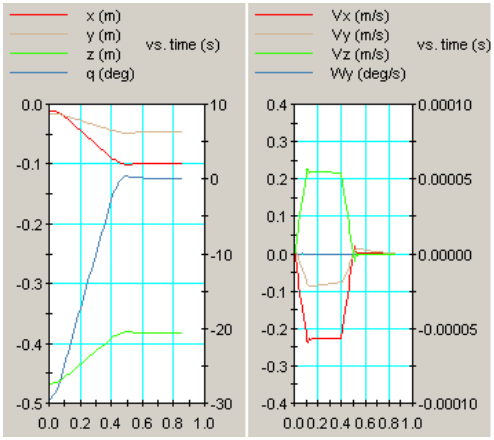

Figure (11) Positions and velocities of the moving platform using Cartesian space control scheme

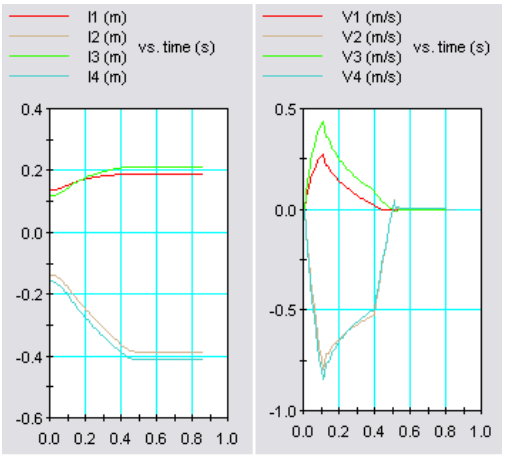

Figure (12) Positions and velocities of the actuated joints using Cartesian space control scheme

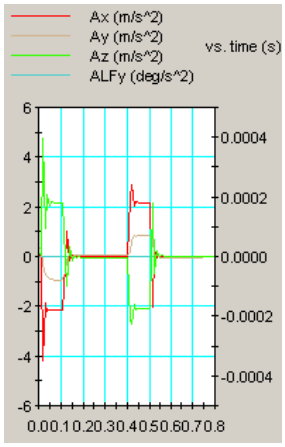

Figure (13) Acceleration of the Platform using Cartesian space control scheme

Similarly, fig. (11) and (12) show the simulation results of the positions and velocities of the moving platform, fig. 11, and of the actuated joints, fig. 12, using the Cartesian space control scheme, fig. 8. The same accuracy as the joint space can be obtained. Fig. 13 shows the acceleration of the platform. This is similar to the acceleration of the trapezoidal velocity profile. Fig. (14) and (15) show the maximum tracking error from Cartesian space control is 4 mm and approximately 2 degree in rotation. Also, maximum platform velocity is 0.2 m/s and that of 0.3g is in acceleration as seen in fig. (13). The error is comparatively small compare to results shown in ref [8]. The error is due to the very high motion with inertia effect which did not include in the controller design but was included in the simulation

5. CONCLUSIONS

In this paper we discuss and analyze theory and possibility of new parallel mechanism design base on H4 family. The forward and inverse kinematics analyses are presented as is singularities analysis. This design show good performance in simulations. We hope to extend the research work to 5-axis machining as well as the rapid prototype application.

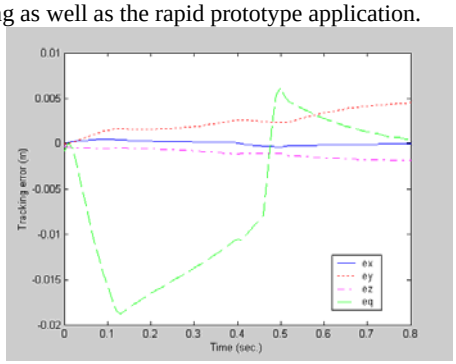

Figure (14) Position tracking error of the moving platform

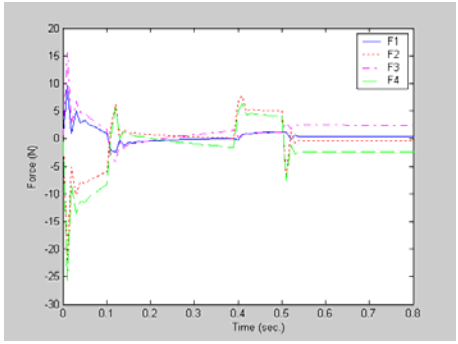

Figure (15) Actuated force for each joint

6. Reference

[1]. Monsarrat, B., Gosselin, C. M. Singularity Analysis of a Three-Leg 6Dof parallel Grassmann Line Geometry. International Journal of Robotics Research vol.20 no.4, April 2001, pp. 312-326.

[2]. Tsai, L. W. Robot Analysis-The Mechanics of Serial and Parallel Manipulators. John Wiley & Sons, 1999.

[3]. Clavel, R., "Conception d'un robot parallèle rapide à 4 degrés de liberté," Ph.D. Thesis, EPFL, Lausanne, Switzerland, 1991.

[4]. Pierrot, F. H4_a new family of 4-DOF parallel robots. IEEE/ASME Advanced Intelligent Mechatronics Conf. Proc. Atlanta USA, September 1999, pp. 508-513.

[5]. Gosselin, C. M., Angeles, J. Singularity analysis of closed-loop kinematics chains. IEEE Transactions on Robotics and Automation vol. 6 no. 3, June, 1990. pp. 281-290.

[6]. Park, K.W., Lee M.K. Workspace and singularity analysis of a double parallel manipulator IEEE/ASME Transactions on Mechatronics vol. 5 no. 4, December 2000, pp. 367-375.

[7]. Chiu, Y.J., Perng, M.H. Forward Kinematics of a General Fully Parallel Manipulator with Auxiliary Sensors. International Journal of Robotics Research vol.20 no.5, May 2001, pp. 401-414.

[8]. Pierrot, F., Marquet, F. H4 parallel robot modeling design and preliminary experiments, IEEE Robotics and Automation Conf. Proc. Seoul Korea, May 2001, pp. 3256-3261.